Indian Journal of Pure & Applied Physics
Vol. 56, October 2018, pp. 792-801

Effect of size and location of solid on conjugate heat transfer in porous cavity

Azeem[a], Irfan Anjum Badruddin[b]*, N Nik-Ghazali[c], Mohd Yamani Idna Idris[d], Ali E Anqi[b], Salman Ahmed N J [e], Sarfaraz Kamangar[b] & Abdullah A A A Al-Rashed[f]

[a]School of Liberal Arts and Social Sciences, Taylors University, No 1 Jalan Taylor's, 47500 Subang Jaya, Selangor Darul Ehsan, Malaysia

[b]Department of Mechanical Engineering, College of Engineering, King Khalid University, PO Box 394, Abha 61421, Kingdom of Saudi Arabia

[c]Department of Mechanical Engineering, University of Malaya, Kuala Lumpur, 50603, Malaysia

[d]Department of Computer System & Technology, University of Malaya, Kuala Lumpur, 50603, Malaysia

[e]Department of Mechanical and Industrial Engineering, Sultan Qaboos University, P O Box 33, Al-Khod, Muscat, 123, Sultanate of Oman

[f]Department of Automotive and Marine Engineering Technology, College of Technological Studies, The Public Authority for Applied Education and Training, Kuwait13092, Kuwait

Received 15 September 2016; accepted 23 April 2018

The highlight of this article is the influence of a solid over heat transfer characteristics in a square porous cavity. The solid placed inside the porous medium is fraction of the whole domain whose size is varied at 5 different locations of the cavity such as left ($\bar{x} = 0$), center ($\bar{x} = 0.5$), right ($\bar{x} = 1$), mid of left and center ($\bar{x} = 0.25$), mid of center and right ($\bar{x} = 0.75$) wall of cavity. The equations that govern the physical phenomenon have been simplified using popular numerical technique such as finite element method. These simultaneous equations are solved for the solution variables such as temperature and the stream function. The physical domain is divided into smaller segments with the help of triangular elements. The left and right vertical surfaces of cavity are maintained at hot and cold temperature T_h and T_c such that $T_h > T_c$.

Keywords: Conjugate heat transfer, Square cavity, Porous medium, Solid wall location

1 Introduction

The advent of computational technology has played a vital role in solving many of the unsolved mathematical problems thus facilitating to understand the complex physical phenomenon which otherwise could have been left unanswered. It can be conveniently said that the advancement in numerical methods as well as computational power of new generation of computers has helped in knowing the conjugate heat transfer in a better way. The advancement in computational methods has particularly helped to solve the multiple set of equations arising due to complex phenomenon and conjugate heat transfer can be categorized as one among those. The relatively simpler phenomenon such as natural convection in porous medium has garnered much attention where various issues related to porous geometry, etc.[1-11] have been investigated and documented in detail. However the complex phenomenon such as conjugate heat transfer is studied relatively to lesser extent. Generally, the conjugate heat transfer is reported for the cases where the solid wall is attached to whole of the surface at one end of geometry under investigation. For instance, the solid wall attached to left wall of cavity is investigated by Saeid[12], Al-Amiri *et al.*[13]. It is reported that the phenomenon of attaining maximum Nusselt number at aspect ratio around 1 vanishes when solid wall is present at the inside radius of vertical annulus[14]. The attachment of two solid walls at parallel surfaces of a porous geometry affects the heat transfer behavior as compared to that of single wall. It was noticed that the average *Nu* almost remains constant for the case when fluid velocity is low owing to low Rayleigh number. The transfer of heat is dominated by conduction in vertical solid walls and porous layer in case of a porous medium placed centrallyin between the solids[15]. A similar geometry was considered by Alhashash[16] to find the influence of radiation and non-uniform heat generation. This study revealed that the

*Corresponding author (E-mail: irfan_magami@rediffmail.com)

heat transfer rate is directly proportional to thickness of solid below a critical thickness of wall. Two solid walls at top and bottom surface of cavity is analyzed by Baytas *et al.*[17] The presence of two solid walls is been studied for other geometries as well. For instance, the effect of varying thermal conductivity of two solids attached at internal and external radii of an annular porous cylinder was investigated to reveal that the influence of conductivity ratio reduced due to enlarged thickness of inner solid and heat transfer rate decreases with increase in the solid conductivity ratio[18]. The heat transfer behavior of triangular porous geometry with solid wall at bottom is reported by Varol *et al.*[19] whereas the triangular solid placed at the bottom corner of a porous cavity was investigated by Chamkha and Ismael[20]. Some of other work in the area of conjugate heat transfer in porous media can be found as inclined vertical plate[21], bi-disperse porous channel[22], porous channel[23], mixed convection coupled with the conjugate heat transfer[24]. A heat source placed at the bottom porous cavity[17], porous medium containing finite horizontal flat plate[25] vertical slender hollow cylinder[26,27], vertical surface in separating two porous media[28] and vertical rounded fin inserted in porous medium [29]. Apart from studying the phenomenon, there have been some attempts to propose new methods to solve the conjugate heat transfer problem[30,31]. It is to be emphasized here that the present work is an extension of our previous work that studied the conjugate double diffusion but present article concentrates purely on heat transfer in the absence of mass transfer. This kind of situation arises in many of the drying processes that get affected due to the presence of a solid object in the porous domain.

2 Mathematical Model

Consider a porous cavity having square shape with a solid wall embedded within the porous region. Figure 1 shows the physical model of problem under investigation. The presence of small solid wall in the porous medium makes it a conjugate heat transfer problem. The height of solid wall is varied in two steps along with its location in five different positions. In first step, the left surface of solid wall coincides with the left surface of cavity, i.e., $\bar{x} = 0$. In the 2nd, 3rd and 4th step, the center of solid wall is placed at 0.25L, 0.5L and 0.75L (25%, 50% and 75% of cavity width). In the last step, the right surface of solid coincides with right surface of cavity. The left and right surface of cavity is isothermally maintained at hot T_h and cool temperature T_c respectively, such that $T_h > T_c$. The standard assumptions are applied such as the applicability of Darcy law, the homogenous properties of medium, etc.

The above problem can be mathematically represented with the help of following four coupled equations as:

$$\frac{\partial u}{\partial x} + \frac{\partial v}{\partial y} = 0 \quad \text{... (1)}$$

$$\frac{\partial u}{\partial y} - \frac{\partial v}{\partial x} = -\frac{g\beta K}{\nu}\frac{\partial T}{\partial x} \quad \text{... (2)}$$

$$u\frac{\partial T_p}{\partial x} + v\frac{\partial T_p}{\partial y} = \alpha\left(\frac{\partial^2 T_p}{\partial x^2} + \frac{\partial^2 T_p}{\partial y^2}\right) - \frac{1}{\rho C_p}\frac{\partial q_r}{\partial x} \quad \text{... (3)}$$

$$\frac{\partial^2 T_s}{\partial x^2} + \frac{\partial^2 T_s}{\partial y^2} - \frac{1}{\alpha\rho C_p}\frac{\partial q_r}{\partial x} = 0 \quad \text{... (4)}$$

The boundary conditions are:

$$u = 0,\ v = 0 \qquad T = T_h \quad at \quad x = 0 \quad \text{... (5a)}$$

$$u = 0,\ v = 0 \qquad T = T_c \quad at \quad x = L \quad \text{... (5b)}$$

$$u = 0,\ v = 0 \qquad \frac{\partial T}{\partial y} = 0 \quad at \quad y=0 \ \textit{and}\ y=L, \quad \text{... (5c)}$$

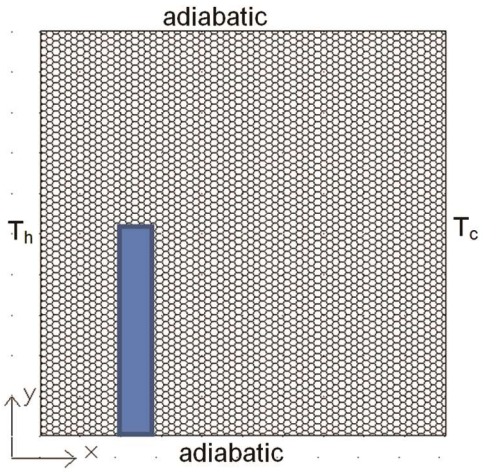

Fig. 1 — Porous cavity with solid at center (3rd position, i.e., 50% of cavity width).

The solid-porous interface needs to satisfy the following condition that arises due to no storage of heat in the medium:

at $x = x_{sp}$ $u = 0,\ v = 0$ $T_s = T_p$

$$k_s \frac{\partial T_s}{\partial x} = k_p \frac{\partial T_p}{\partial x} \quad \text{... (5d)}$$

at $y = y_{sp}$ $u = 0,\ v = 0$ $T_s = T_p$

$$k_s \frac{\partial T_s}{\partial y} = k_p \frac{\partial T_p}{\partial y} \quad \text{... (5e)}$$

Stream function ψ is introduced as:

$$u = \frac{\partial \psi}{\partial y} \quad \mathrm{v} = -\frac{\partial \psi}{\partial x} \quad \text{... (6)}$$

The non-dimensional parameters are:

$$\bar{x} = \frac{x}{L}, \quad \bar{y} = \frac{y}{L}, \ \bar{\psi} = \frac{\psi}{\alpha},$$

$$\bar{T} = \frac{(T - T_c)}{(T_h - T_c)}, \ Rd = \frac{4\sigma T_c^{\,3}}{\beta_r k}, \ Ra = \frac{g\beta\ \Delta TKL}{\nu\alpha}$$

Making use of Rossel and approximation to represent the radiation heat transfer in the domain[1] yields:

$$q_r = -\frac{4\sigma}{3\beta_r}\frac{\partial T^4}{\partial x} \quad \text{... (7)}$$

The term T^4 in above equation can be expanded through Taylor series about T_c [1,32-39] as:

$$T^4 \approx 4TT_C^{\,3} - 3T_C^{\,4} \quad \text{... (8)}$$

Substituting Eqs (6-8) into Eqs (2-4) yields:

$$\frac{\partial^2 \bar{\psi}}{\partial \bar{x}^2} + \frac{\partial^2 \bar{\psi}}{\partial \bar{y}^2} = -Ra\frac{\partial \bar{T}_p}{\partial \bar{x}} \quad \text{... (9)}$$

$$\left[\frac{\partial \bar{\psi}}{\partial \bar{y}}\frac{\partial \bar{T}}{\partial \bar{x}} - \frac{\partial \bar{\psi}}{\partial \bar{x}}\frac{\partial \bar{T}}{\partial \bar{y}}\right] = \left(\left(1 + \frac{4R_d}{3}\right)\frac{\partial^2 \bar{T}}{\partial \bar{x}^2} + \frac{\partial^2 \bar{T}}{\partial \bar{y}^2}\right) \quad \text{... (10)}$$

$$\left(1 + \frac{4R_d}{3}\right)\frac{\partial^2 \bar{T}}{\partial \bar{x}^2} + \frac{\partial^2 \bar{T}}{\partial \bar{y}^2} = 0 \quad \text{... (11)}$$

The corresponding boundary conditions are:

at $\bar{x} = 0$ $\bar{\psi} = 0$ $\bar{T} = 1$ ... (12a)

at $\bar{x} = 1$ $\bar{\psi} = 0$ $\bar{T} = 0$ ... (12b)

at $\bar{y} = 0$ *and* $\bar{y} = 1,\ \bar{\psi} = 0$ $\frac{\partial \bar{T}}{\partial \bar{y}} = 0$ ... (12c)

at $\bar{x} = x_{sp}$ $\bar{\psi} = 0,$ $Kr\frac{\partial \bar{T}_s}{\partial \bar{x}} = \frac{\partial \bar{T}_p}{\partial \bar{x}}$ ⋯ (12d)

at $\bar{y} = \bar{y}_{sp}$ $\bar{\psi} = 0$ $Kr\frac{\partial \bar{T}_s}{\partial \bar{y}} = \frac{\partial \bar{T}_p}{\partial \bar{y}}$ ⋯ (12e)

3 Numerical Method

The above mentioned Eqs (9-11) are complex partial differential equations subjected to intricate boundary conditions (12) that are difficult to solve directly. In the present case, they are solved by making use of finite element method. The whole domain is divided into smaller segments known as elements of triangular shape. The number of element in finite element method plays a role in varying the accuracy of results. Thus the present methodology adopted to divide the porous domain into sufficient number of elements (2592) which ensured that the results are not significantly affected beyond this number of elements. The application of finite element method transforms Eqs (9-11) into huge number of algebraic form of equations, equivalent to the number of nodes in the domain. The resulting equations are solved for $\bar{T}$ *and* $\bar{\psi}$ by setting the convergence criteria as 10^{-9} and 10^{-6} for $\bar{\psi}$ *and* $\bar{T}$ respectively. Any adopted method should prove its applicability in reproducing the standard results which validates the

procedure being adopted. Thus the current method is validated by diminishing the thickness of wall that corresponds to square porous cavity. Table 1 shows the comparison which clearly vindicates the accuracy of present method. The Nu can be represented as:

$$Nu = -\left(\left(1+\frac{4}{3}R_d\right)\frac{\partial \overline{T}}{\partial \overline{x}}\right)_{\overline{x}=0} \quad \ldots\cdot(13)$$

Average *Nu*:

$$\overline{Nu} = \int_0^1 Nu.d\overline{y} \quad \ldots (14)$$

4 Results and Discussion

The following section describes the Nusselt number behavior at hot surface of cavity with respect to the location of solid inside the domain and thermal conductivity ratio. The position of solid is considered from hot surface to cold surface. Four different size of solid height (S_h = 10%, S_h =20%, S_h =30% and S_h =50% of cavity height) and 2 values of solid width (S_w =13% and S_w =25% of cavity width) are analyzed. Figure 2 shows the variations in heat transfer represented by Nusselt number *Nu,*when solid occupies the place at $\bar{x} = 0.25$ for *Ra*=100 *and* R_d =0.5. It is obvious from Fig. 2 that the Nusselt number for S_w=0.13 (13%) increases initially up to a pint with respect to increase in *Kr* but afterwards the variation is seized. However, the Nusselt number keeps increasing with increase in *Kr* for wider solid (S_w=0.25). This is due to the fact that the wider solid width imposes greater thermal resistance as compared to smaller solid. However increase in *Kr* which is reflection of enhanced thermal conductivity of solid, reduces the thermal resistance, thus increasing the Nusselt number. The increased conductivity ratio increases the temperature gradient at hot surface leading to increased heat transfer rate. In general, the *Nu* for shorter solid height is higher than that of longer solid at smaller *Kr* with exception of S_h=0.1. This is due to the reason that the longer solid obstructs the fluid movement to greater extent thus rendering the overall heat transfer capacity of fluid.

Figure 3 shows the average *Nu* when solid is placed at the center of cavity with other parameters being same as that of Fig. 2. It is seen that the shifting of solid from $\bar{x} = 0.25$ to $\bar{x} = 0.5$, which is the center of cavity, results into higher Nusselt number for shorter solid width as compared to larger width for all values of *Kr* being investigated. This could be attributed to increased fluid velocity due to lesser resistance in the vicinity of hot surface. The attainment of maximum $\overline{Nu}$ shifts towards smaller *Kr* when location of solid is moved from $\bar{x} = 0.25$ to $\bar{x} = 0.5$.

Table 1 — Comparison of results

Literature	Ra=10	Ra=100
Gross *et al.*[40]		3.141
Bejan[41]		4.2
Walker and Homsy[42]		3.097
Beckerman *et al.*[43]		3.113
Monolo and Lage[44]		3.118
Misirlioglu *et al.*[45]	1.119	3.05
Moya *et al.*[46]	1.065	2.801
Baytas and Pop[47]	1.079	3.16
Present study	1.0821	3.2126

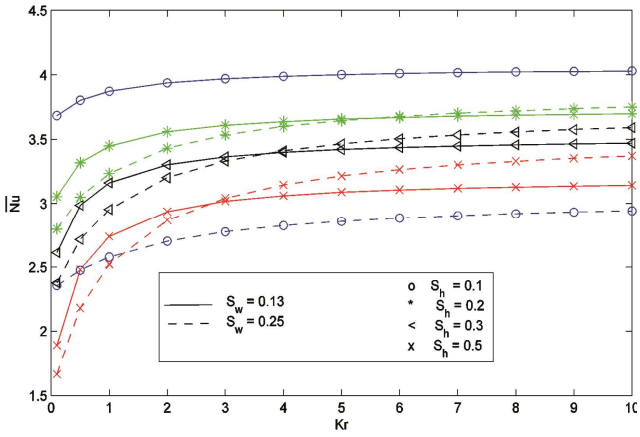

Fig. 2 — Average Nusselt number variation with *Kr* for solid at $\bar{x} = 0.25$.

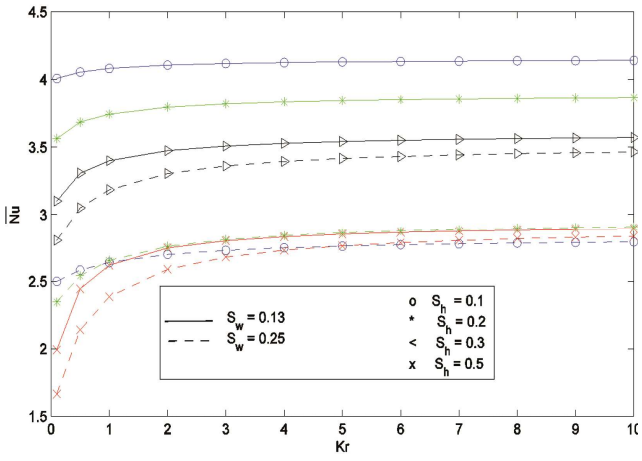

Fig. 3 —Average Nusselt number variation with *Kr* for solid at $\bar{x} = 0.5$.

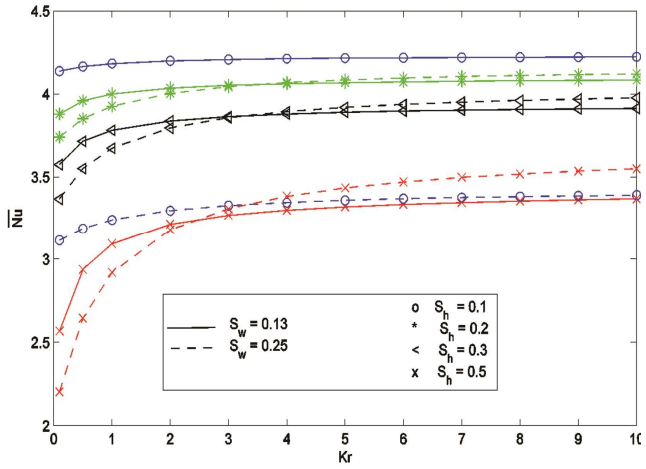

Fig. 4 — Average Nusselt number variation with *Kr* for solid at $\bar{x} = 0.75$.

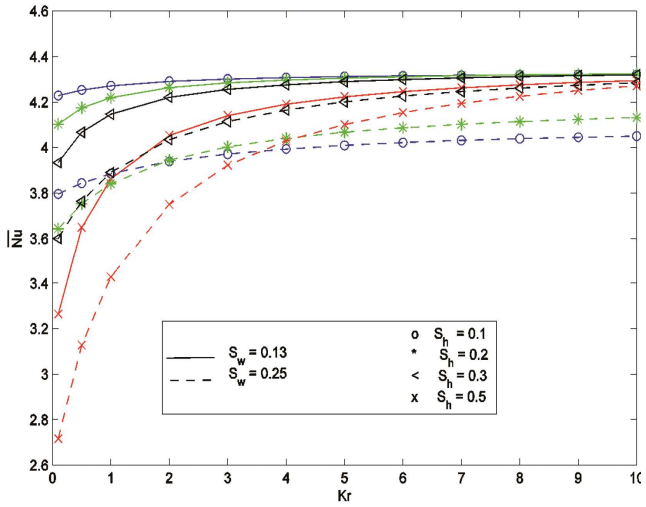

Fig. 5 — Average Nusselt number variation with *Kr* for solid at $\bar{x} = 1$ (cold surface).

Figure 4 shows the effect of solid being placed at $\bar{x} = 0.75$, keeping all other parameters same as previous case, i.e., Fig. 2. The heat transfer increased by pushing the solid towards right surface. The average *Nu* for wider solid is higher at larger *Kr* value. The average *Nu* further increases due to further moving of the solid towards the cold surface of cavity, as shown in Fig. 5. This behaviour is a result of higher fluid velocity at hot surface due to lesser obstruction posed by solid wall. The higher velocity fluid carries more amount of heat from hot surface thus increasing the average *Nu*. The effect of *Kr* on heat transfer rate is substantial for S_h=0.5 as compared to other values of S_h.

Figure 6 depicts the isotherms and streamlines when the solid is placed at 25% of cavity width with *Ra*=100, R_d=0.5, S_h=0.20 and different values of thermal conductivity ratio, i.e., *Kr*=0.1, 1 and 10. It is seen that the increase in the thermal conductivity ratio increases the thermal gradient from solid to porous region as indicated by isotherms being closer to hot surface at higher value of *Kr*. The isotherms are clustered near the solid wall for low value of thermal conductivity ratio (*Kr*=0.1) but it spreads out of solid wall owing to increased thermal conductivity ratio. The fluid flow direction also tilts to vertical as compared to being nearly horizontal at *Kr*=0.1. It is seen that the fluid gets obstructed due to presence of solid wall inside the porous medium and that region is occupied with crowded streamlines. The strength of streamlines increases due to increase in thermal conductivity ratio which further vindicates that the heat transfer should increase due to increase of *Kr*

Figure 7 shows the isotherms and streamlines when solid wall is placed exactly at the center of cavity. It is interesting to note that the solid wall attains more uniformity in temperature as compared to the earlier case which is evident from Fig. 7 that shows fewer isotherms (Fig. 7(a)) inside the solid as compared to 10 isotherms of previously discussed cases (Fig. 6(a)). The strength of streamlines is stronger when solid is placed at the center. This could be due to the reason that the fluid does have sufficient space to gain momentum before it encounters the obstruction of solid compared to other cases. The solid temperature varies considerably when the S_h is 50% at center of cavity, as illustrated in Fig. 7. The flow is concentrated more on left side of cavity at smaller value of *Kr* but it tries to attain uniformity across cavity when *Kr* increases. The fluid cell breaks into two separate flow regions when conductivity of solid increases.

The variation of temperature in solid wall further decreases when its location is moved towards right wall of cavity as obvious from Fig. 8 that the maximum and minimum temperature is just 0.3 and 0.1, respectively, within the solid wall. The fluid flow strength further increases when solid is moved farther away from left wall. This can be attributed to the fact that the fluid has sufficient space before encountering the obstruction that that allows the fluid to gain momentum.

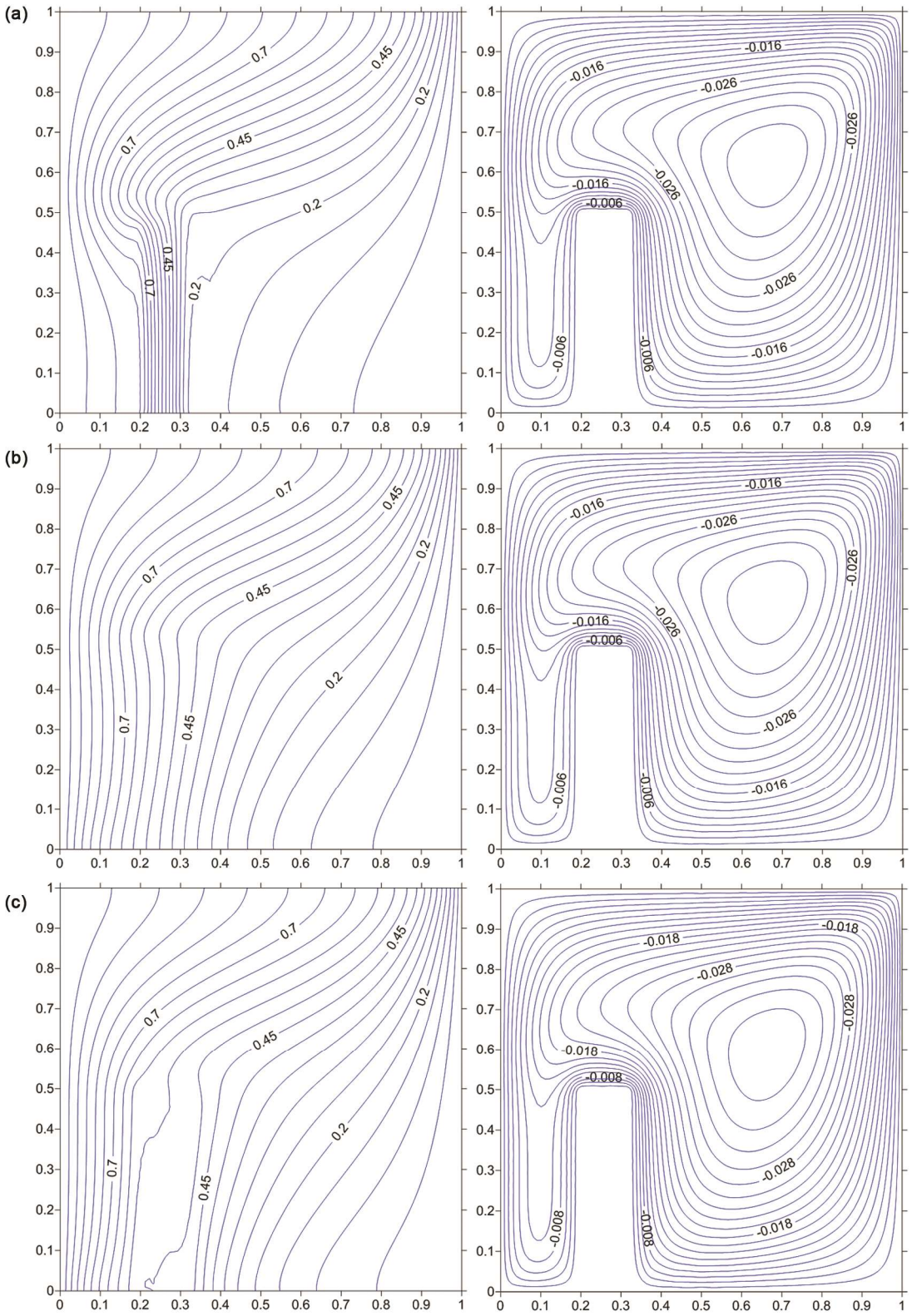

Fig. 6 — Isotherms (left) and streamline (right) when solid wall placed at L=0.25 for S_h=0.5 (a) Kr=0.1, (b) Kr=1 and (c) Kr=10.

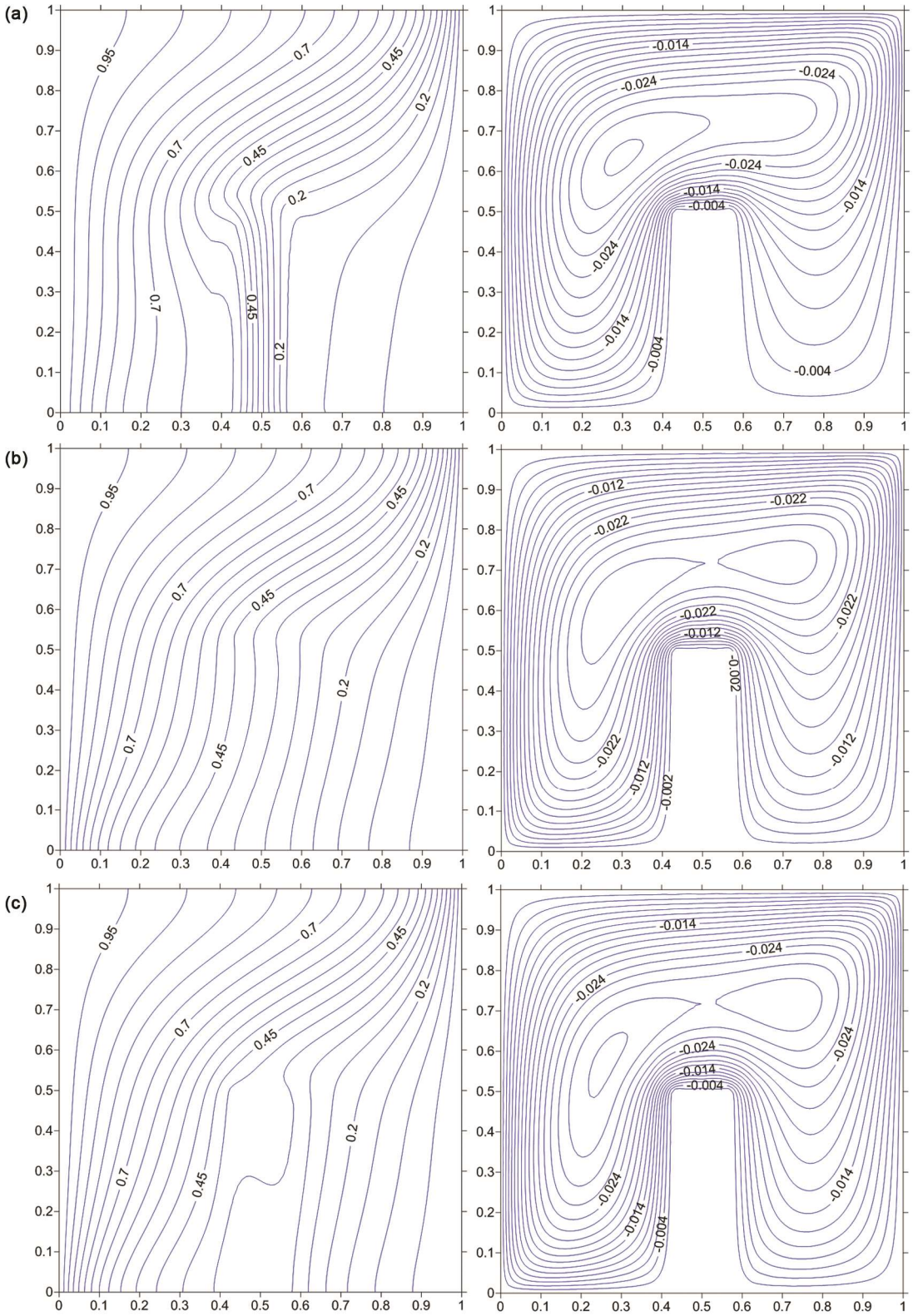

Fig. 7 — Isotherms (left) and streamline (right) when solid wall placed at L=0.5 for S_h=0. 5 (a) Kr=0.1, (b) Kr=1 and (c) Kr=10.

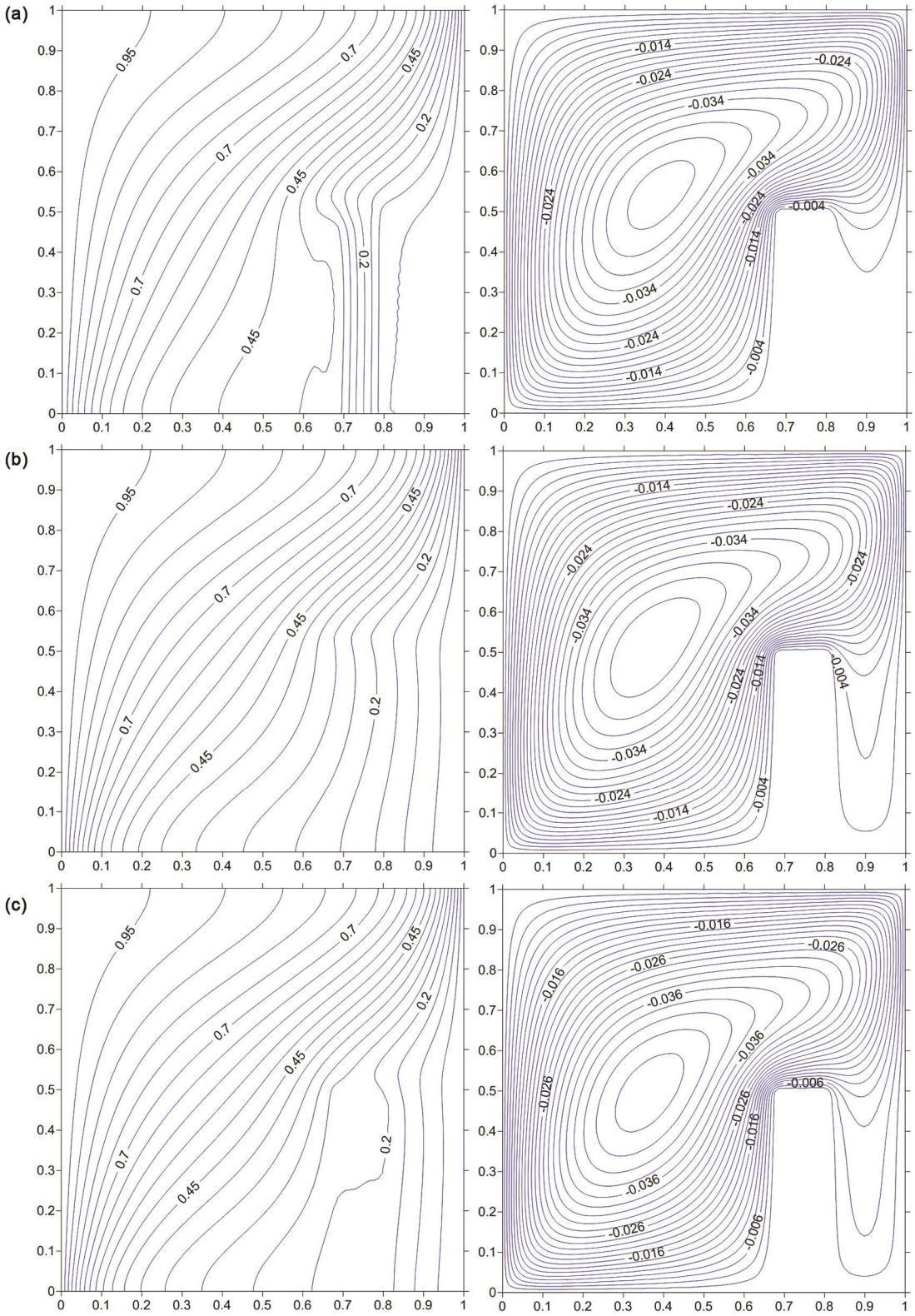

Fig. 8 — Isotherms (left) and streamline (right) when solid wall placed at L=0.75 for S_h=0.5 (a) Kr=0.1, (b) Kr=1 and (c) Kr=10.

5 Conclusions

The present work investigates the conjugate heat transfer inside a square porous cavity. Emphasis is given to understand the heat and fluid flow behavior when the conductivity ratio and location of solid wall is varied. The following conclusion can be drawn from this work:

(i) The increased conductivity ratio increases the heat transfer rate in the cavity due to decrease in overall thermal resistance.
(ii) Fluid flow strength decreases with increase in the solid wall height because of increased obstruction but increase with increased conductivity ratio.
(iii) Temperature variations inside the solid wall keep decreasing as its position is moved towards the cold surface of cavity leading to higher Nusselt number.
(iv) The fluid velocity increases with moving the solid wall towards the cold surface.
(v) Average Nusselt number increase with increase in thermal conductivity ratio.
(vi) Generally, the variation in Nusselt number is substantial at smaller values of *Kr*.

Acknowledgement

The authors extend their appreciation to the Deanship of Scientific Research at King Khalid University for funding this work through research groups program under grant number (R.G.P.1/29/38).

Nomenclature

C_p	Specific heat of fluid (J/kg-^{o}C)
g	Acceleration due to gravity (m/s^2)
k	Thermal conductivity (W/m-^{o}C)
k_p ,k_s	Porous and solid thermal conductivity respectively (W/m-^{o}C)
K	Permeability of porous medium (m^2)
Kr	Conductivity ratio
L	Height and length of cavity (m)
Nu, $\overline{Nu}$	Local Nusselt number and average Nusselt number, respectively
q_r	Radiation flux (W/m^2)
R_d	Radiation parameter
Ra	Modified Raleigh number
S_w	Solid width
S_h	Solid height
$T, \overline{T}$	Dimensional (^{o}C) and non-dimensional temperature
u, v	Velocity components in x and y direction, respectively (m/s)
x, y	Cartesian co-ordinates
$\overline{x}, \overline{y}$	Non-dimensional co-ordinates
	Greek Symbols
α	Thermal diffusivity (m^2/s)
β	Coefficient of thermal expansion (1/^{o}C)
ρ	Density (kg/m^3)
ν	Coefficient of kinematic viscosity(m^2/s)
σ	Stephan Boltzmann constant (W/m^2-K^4)
β_r	Absorption coefficient (1/m)
ψ	Stream function
$\overline{\psi}$	Non-dimensional stream function
	Subscripts
h	Hot
c	Cold
p	Porous
s	Solid
sp	solid-porous interface

References

1 Raptis A, *Int Commun Heat Mass Transfer*, 25 (1998) 289.
2 Ahmed N J S, Badruddin I A, Zainal Z A, Khaleed H M T & Kanesan J, *Int J Heat Mass Transfer*, 52 (2009) 3070.
3 Ahmed N J S, Badruddin I A, Kanesan J, Zainal Z A & Ahamed K S N, *Int J Heat Mass Transfer*, 54 (2011) 3822.
4 Badruddin I A, Abdullah A A A A, Ahmed N J S & Kamangar S, *Int J Heat Mass Transfer*, 55 (2012) 2184.
5 Ogulu A & Amos E, *Int Commun Heat Mass Transfer*, 32 (2005) 974.
6 Badruddin I A, Ahmed N J S, Al-Rashed A A A A, Kanesan J, Kamangar S & Khaleed H M T, *Transport Porous Media*, 91 (2012) 697.
7 Badruddin I A, Al-Rashed A A A A, Ahmed N J S, Kamangar S & Jeevan K, *Int J Heat Mass Transfer*, 55 (2012) 7175.
8 Kumaran V & Pop I, *Int J Heat Mass Transfer*, 49 (2006) 3240.
9 Badruddin I A, Khan T M Y, Salman A N J & Kamangar S, *AIP Conf Proc*, 1728 (2016) 020689.
10 Badruddin I A & Quadir G A, *AIP Conf Proc*, 1738 (2016) 480127.
11 Badruddin I A & Quadir G A, *AIP Conf Proc,* 1738 (2016) 480126.
12 Saeid N H, *Int J Thermal Sci*, 46 (2007) 531.
13 Al-Amiri A, Khalil K & Pop I, *Int J Heat Mass Trans*, 51 (2008) 4260.
14 Ahmed N J S, Kamangar S, Badruddin I A, Al-Rashed A A A A, Quadir G A, Khaleed H M T & Khan T M Y, *J Porous Media*, 19 (2014) 1109.
15 Saeid N H, *Int Comm Heat Mass Transfer*, 34 (2007) 210.
16 Alhashash A, Saleh H & Hashim I, *Transport Porous Media*, 99 (2013) 453.
17 Baytas A C, Liaqat A, Groşan T & Pop I, *Heat Mass Transfer*, 37 (2001) 467.

18 Badruddin I A, Ahmed N J S, Al-Rashed A A A A, Ghazali N N, Jameel M, Kamangar, S, Khaleed H M T & Khan T M Y, *Transport Porous Media*, 109 (2015) 589.
19 Varol Y, Oztop H F & Pop I, *Int J Numer Meth Heat Fluid Flow*, 19 (2009) 650.
20 Chamkha A J & Ismael M A, *Numer Heat Transfer*, 63(2013) 144.
21 Ali F, Khan I & S Shafie, S, *PLoS ONE*, 8 (2013) e65223.
22 Nield D A & Kuznetsov A V, *Int J Heat Mass Transfer*, 47 (2004) 5375.
23 Mahmud S E & Fraser R A, *Heat Mass Transfer*, 41 (2005) 568.
24 Pop I & Merkin J H, *Fluid Dyn Res*, 16 (1995) 71.
25 Aleshkova I A & Sheremet M A, *Int J Heat Mass Transfer*, 53 (2010) 5308.
26 Pop I & Na T Y, *Heat Mass Transfer*, 36 (2000) 375.
27 Ahmet K, *Int J Heat Mass Transfer*, 54 (2011) 31818.
28 Vaszi A Z, Elliott L, Ingham D B & Pop I, *Int J Heat Mass Transfer*, 45 (2002) 2777.
29 Vaszi A Z, Elliott L, Ingham D B & Pop I, *Int J Heat Mass Transfer*, 47 (2004) 2785.
30 Badruddin I A, Azeem K Idna Idris MY, Nik-Ghazali N, Salman Ahmed N J & Abdullah A A A A, *Int J Numer Meth Heat Fluid Flow*, 27 (2017) 2481.
31 Sheng C, *Int J Therm Sci*, 124 (2018) 477.
32 Badruddin I A, Zainal Z A, Narayana P A, Seetharamu K N & Siew L W, *Int J Therm Sci*, 45 (2006) 487.
33 Badruddin I A, Zainal Z A, Narayana P A, Seetharamu K N & Siew L W, *Int J Numer Meth Eng*, 65 (2006) 2265.
34 Badruddin I A, Zainal Z A, Narayana P A, Seetharamu, KN, *Int comm Heat Mass Trans*, 33 (2006) 491.
35 Ghazali, N N, Badruddin, I A, Badarudin A & Tabatabaeikia S, *Adv Mech Eng*, 6 (2014) 209753.
36 Badruddin I A, Zainal Z A, Khan Z A & Mallick Z, *Int J Therm Sci*, 46 (2007) 221.
37 Badruddin I A, Zainal Z A, Narayana P A & Seetharamu K N, *Int Commun, Heat Mass Transfer*, 33 (2006) 500.
38 Badruddin I A, Zainal Z A, Narayana P A & Seetharamu K N, *Int J Therm Sci*, 46 (2007) 20.
39 Badruddin I A, Zainal Z A, Narayana P A & Seetharamu K N, *Int J Heat Mass Transfer*, 49 (2006) 4955.
40 Gross R J, Bear M R & Hickox C E, *Proceedings of 8th Int Heat Transfer Conf San Francisco*, CA, USA, 1986.
41 Bejan A, *Lett Heat Mass Transfer*, 6 (1979) 93.
42 Walker K L, Homsy, *J Fluid Mech*, 87 (1978) 449.
43 Bekermann C, Viskanta R & Ramadhyani S, *Numer Heat Transfer Part A*, 10 (1986), 557.
44 Manole D M & Lage J L, *ASME Conference*, 55 (1992) 216.
45 Misirlioglu A, Baytas A C & Pop I, *Int J Heat Mass Trans*, 48 (2005) 1840.
46 Moya S L, Ramos E & Sen M, *Int J Heat Mass Trans*, 30 (1987) 741.
47 Baytas A C & Pop I, *Int J Heat Mass Trans*, 42 (1999) 1047.